International Journal of Structural Analysis & Design – IJSAD
Volume 1: Issue 2 [ISSN: 2372-4102]
Publication Date : 25 June 2014

Evaluation of Current Strut-and-Tie Design Provisions for Deep Beams by a Concrete Limit Analysis

[Jin-Woo Kim, Sung-Gul Hong, Young Hak Lee, Heecheul Kim and Dae-Jin Kim*]

***Abstract*— The current American Concrete Institute (ACI), Canadian Standard Associate (CSA) and CEB-FIP code provisions suggest that deep beams should be designed using the strut-and-tie model approach. This paper investigates the validity of the current ACI, CSA and CEB-FIP code provisions on the shear strength of simply supported reinforced concrete deep beams by comparing them with the shear strength equations proposed by Hong et al. [1] The comparison shows that the current ACI and CEB-FIP design codes can provide reasonable shear strength estimates that approximately correspond to the 70 to 80 % of the predictions by the shear strength equations. In contrast, the current CSA code relatively underestimates the shear strength for cases with large shear-span ratio.**

***Keywords*—strut-and-tie model; concrete deep beam; shear strength; concrete plasticity.**

I. Introduction

Reinforced concrete deep beams are generally defined as a beam member with shear span ratio less than two. They have many applications such as load transfer girders, wall footings and shear walls. The structural behavior of reinforced concrete deep beams is mainly governed by the flow of shear force in the member and their ultimate strengths are generally well predicted by the limit analysis based on concrete plasticity such as strut-and-tie models.

The current concrete design codes such as ACI 318-11 [2], CSA A.23.3-04 [3] and CEB-FIP Model Code 2010 provisions [4] on the shear strength of a simply supported deep beam and its end anchorage details suggest that deep beams should be designed using the strut-and-tie model. The strut-and-tie model is a design methodology based on the lower bound theorem of concrete limit analysis. It allows designers to create proper strut-and-tie models for members with geometric or static discontinuities and to provide steel reinforcement in accordance with its detailing requirements. Although this is a useful methodology to design members in disturbed regions (D region), the quality of the design is highly dependent on the truss model that designers create.

Jin-Woo Kim/ Young Hak Lee/ Heecheul Kim/ Dae-Jin Kim* (*: Corresponding author)
Department of Architectural Engineering/ Kyung Hee University
Republic of Korea

Sung-Gul Hong
Seoul National University
Department of Architecture/ Seoul National University
Republic of Korea

In order to accurately estimate the shear strength of concrete deep beams with the consideration of end anchorage failure, Hong et al. [1] derived the shear strength equations of reinforced concrete deep beams. They are based on the upper bound theorem in the theory of plasticity, and several realistic failure mechanisms are considered. The validity of these equations was investigated through experimental work, and it showed that the proposed equations are able to accurately predict the shear strength of a RC deep beam and its associated failure mechanism. Therefore, in this paper, we investigate the validity of the three current concrete design codes, which are ACI 318-11, CSA A.23.3-04 and CEB-FIP Model Code 2010, on these issues by comparing the estimates by the code with those of the strength equations by Hong et al.

II. Current Design Provisions and Shear Strength Equations

A. *Failure mechanisms and shear strength equations*

This section summarizes the shear strength equations of reinforced concrete (RC) deep beams that were derived by Hong et al. [1] and their associated failure mechanisms. Figure 1 presents the five failure mechanisms considered in [1] to realistically describe possible failure modes of RC deep beams where end anchorage failures may be involved. Two of them have nothing to do with anchorage failure; one associated with concrete web crushing and longitudinal bar yielding failure (S) and the other associated with pure flexural failure (F). The other three failure mechanisms are controlled by end anchorage failure of longitudinal bars in combination with concrete web crushing (A1), concrete diagonal tension failure (A2) and flexural failure (A3). The shear strengths of the deep beams associated with each type of failure mechanism are also provided in Figure 1, and they were derived based on the upper bound theorem of the plasticity theory. Consequently, the smallest one among the shear strength values predicted by these equations is closest to the exact solution. Since a small size bearing plate may cause a premature concrete crushing failure near the region of the support, the size of the bearing plate is also considered in the derivation of these equations.

B. *Current strut-and-tie design provisions*

Currently, most of concrete design provisions such as ACI 318-11, CSA A.23.3-04 and CEB-FIP Model Code 2010

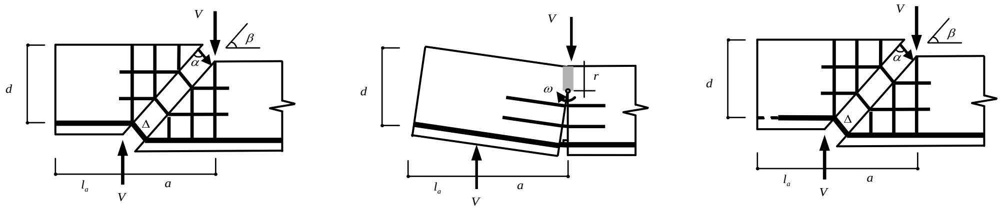

$$\frac{\tau_u^*}{f_c'} = \frac{1}{\sin(\alpha+\beta)}[-\Phi\cdot\cos(\alpha+\beta) + \frac{\nu}{2}\frac{(1-\sin\alpha)}{\sin\beta} + \Psi_v\cdot\cot\beta\sin(\alpha+\beta) - \Psi_h\cdot\cos(\alpha+\beta)] \quad \text{(1: S)}$$

$$\frac{\tau_u}{f_c'} = \frac{d}{2a}\cdot\frac{2\nu_c\Phi-\Phi^2+\nu_c\Psi_h}{\nu_c+\Psi_h} \quad \text{(2: F)}$$

$$\frac{\tau_u^*}{f_c'} = \frac{1}{\sin(\alpha+\beta)}[\lambda_s(\lambda_a+\frac{a}{d}-\cot\beta) + \frac{\nu}{2}\frac{(1-\sin\alpha)}{\sin\beta} + \Psi_v\cdot\cot\beta\sin(\alpha+\beta) - \Psi_h\cdot\cos(\alpha+\beta)] \quad \text{(3: A1)}$$

$$\frac{\tau_u^*}{f_c'} = \frac{d}{a}\left[\lambda_s\left(\lambda_a+\frac{a}{d}-\cot\beta\right)+\frac{1}{2}\cot^2\beta\cdot\Psi_v+\frac{1}{2}\Psi_h\right] \quad \text{(4: A2)}$$

$$\frac{\tau_u}{f_c'} = \frac{d}{2a}\cdot\frac{2\nu_c\lambda_s(\lambda_a+\frac{a}{d})-\lambda_s^2(\lambda_a+\frac{a}{d})^2+\nu_c\Psi_h}{\nu_c+\Psi_h} \quad \text{(5: A3)}$$

Figure 1. Failure mechanisms and shear strength equations. [1]

TABLE I. CURRENT STRUT-AND-TIE DESIGN PROVISIONS.

	ACI 318-11	CSA A.23.3-04	CEB-FIP Model Code 2010
Strut strength	$F_{ns}=(0.85\beta_s f'_c)bw_{st}$	$F_{ns}=f'_c A_c$	$f_{cd1}=1.0\left[\frac{30}{f_{ck}}\right]^{1/3}$ for non-cracked zone
		$\phi F_{ns}=\phi_c f_{cu} A_{cs}$ $f_{cu}=\frac{f'_c}{0.8+170\varepsilon_1}\le 0.85 f'_c$	$f_{cd2}=0.75\left[\frac{30}{f_{ck}}\right]^{1/3}$ for cracked zone
Requirement for main reinforcement	$F_{nt}=A_{st}f_y\ge F_u$	$F_{nt}=f_y A_{st}$	$f_{ytd}=f_{ytk}$
Nodal effectiveness factor	CCC = 1.0 CCT = 0.8 CTT = 0.65	CCC = 0.85 CCT = 0.75 CTT = 0.65	Effective strength of CCC nodes = f_{cd1} Effective strength of CCT or CTT nodes = f_{cd2}

suggest that the deep beams should designed based on the strut-and-tie model. The main components, of which strengths must be checked during the process of the strut-and-tie design, include concrete struts, tie reinforcements and nodal zones. The requirements for these components are summarized in Table I. It reveals that the occurrence of cracking affects the strength of a concrete strut in the current ACI and CEB-FIP codes while the angle of the concrete strut is the most critical factor to determine its strength in the current CSA code. The requirements for the main reinforcement are basically identical in all three design codes. In the estimation of nodal zone strength, the application of tensile force to the node generally reduces its effective strength. Thus, CCC nodes have the highest effectiveness factor, and CTT nodes the lowest. Based on this principle, the current ACI and CSA codes suggest predetermined effectiveness factors for different types of nodal zones as given in the table. The current CEB-FIP code uses the nodal zone strength equations, which are the same as those used for concrete struts.

III. Comparison of Estimates by the Current Design Provisions and Shear Strength Equations

This section describes the methodology to compare the three current design code provisions and the shear strength equations introduced in the previous section. For this comparison, a representative deep beam example is chosen, and it is illustrated in Figure 2. The material properties and geometric dimensions are listed in Table II. The simple single-span truss model shown in Figure 3 is used to estimate the shear strength of the representative example based on the three current code provisions. In this procedure, the shear strength is defined as the smallest applied load (V_u) when the internal force of any strut or tie component in the truss model reaches its own strength determined by the design codes. The ratio between the widths of the upper horizontal strut and lower horizontal tie is fixed as 0.8 from the horizontal force equilibrium condition. For fair comparison between the code estimates and predictions by the shear strength equations, any kind of safety factors provided by the current design codes are not considered. The representative example is designed so that it can satisfy the end anchorage requirements of all of the three current design codes. Therefore, premature end anchorage failures are prevented in this example.

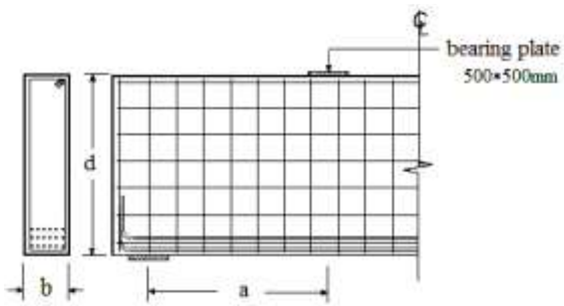

Figure 2. Details of the representative model.

TABLE II. MATERIAL PROPERTIES AND GEOMETRIC DIMENSIONS OF THE REPRESENTATIVE EXAMPLE.

f'_c	27 MPa
f_y	400 MPa
b	500 mm
A_s	9100 mm^2
Horizontal and vertical shear reinforcement	D13(mm) @ 250(mm)

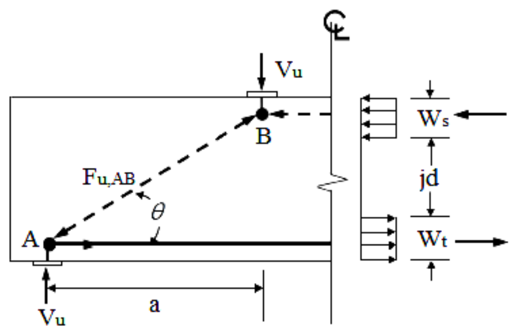

Figure 3. Single-span truss model.

IV. Analysis of the Results

In this section, the shear strength predictions by the three current code provisions are compared with those of the shear strength equations for the representative example introduced in the previous section. The comparison is done in terms of the shear-span ratio (a/d), the aspect ratio of the cross section and the amount of main reinforcement (A_s).

Figure 4 shows the shear strength curves that are estimated by the three current design codes and the shear strength equations for shear-span ratios ranging from 0.6 to 1.5. The amount of main reinforcement is 7,800 mm^2, and the depth of the beam is 2,500 mm for all these cases. Since the shear strength equations are derived based on the upper bound theorem of the concrete plasticity, the smallest shear strength among the values provided by the four failure mechanisms (S, F, A1 and A2) can be regarded as the strength determined by the shear strength equation for a given shear-span ratio. The figure indicates that the shear failure mechanism (S) is the governing failure mechanism approximately up to the shear-span ratio of 0.7 while the flexural failure mechanism (F) becomes the governing mechanism beyond that shear-span ratio. This coincides with the general expectation on the failure mode of concrete deep beams with respect to the shear-span ratio.

The shear strengths estimated by the three current design provisions are plotted as piecewise linear functions in the figure. They show a trend similar to the predictions by the shear strength equations, but their values are smaller than those by the shear strength equations. In order to investigate their accuracy, these strength values are divided by the estimated valuea by the shear strength equations, and the ratios are listed in Table III. The results in the table indicate that the predictions by the ACI and CEB-FIP codes are in the range of approximately 70 to 80 %, which is reasonable. In contrast, the CSA code relatively underestimates the shear strength for cases with large shear-span ratio. This seems because the effective strut strength of the CSA code is greatly reduced as the shear-span ratio increases.

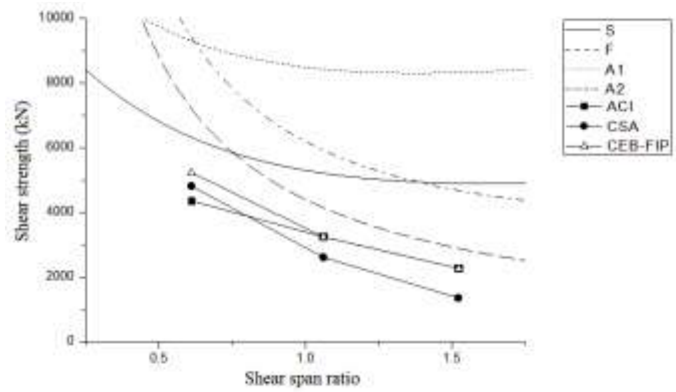

Figure 4. Shear strengths of the representative example estimated by the three current design codes and the shear strength equations for different shear-span ratios.

TABLE III. RATIOS BETWEEN THE SHEAR STRENGTHS PREDICTED BY THE THREE CURRENT CODE PROVISIONS AND THE SHEAR STRENGTH EQUATIONS FOR THREE DIFFERENT SHEAR-SPAN RATIOS.

Shear-span ratio	**0.6**	**1.0**	**1.5**
ACI	68.9 %	75.4 %	75.5 %
CSA	80.5 %	71.0 %	53.0 %
CEB-FIP	81.2 %	75.4%	75.5 %

Figure 5 shows the ratios between the shear strengths predicted by the three current code provisions and the shear strengths equations for three different depths, which are 2,500 mm, 3,000 mm and 3,500 mm. The amount of main reinforcement is 9,100 mm^2, and the shear-span ratio is 1.0 for all these cases. The results of the figure are also listed in Table IV. This analysis is done to investigate the effect of the aspect ratio of the beam cross section on the shear strength. The results in the figure and table indicate that the ratio decreases as the beam depth increases. For example, in the case of the ACI code, the ratio decreases from 82.1 % to 75.3 % as the beam depth increases from 2,500 mm to 3,500 mm. This seems mainly because the area of the inclined concrete strut does not increase as much as the beam depth increases, thus the overall shear strength does not increase. Furthermore, the contributions of horizontal and vertical shear reinforcement are not well considered in the single-span truss model, on which the estimation by the current code provisions is based. Therefore, a more realistic and complicated truss model than the single-span model may be required to capture the effect of aspect ratio on the shear strength.

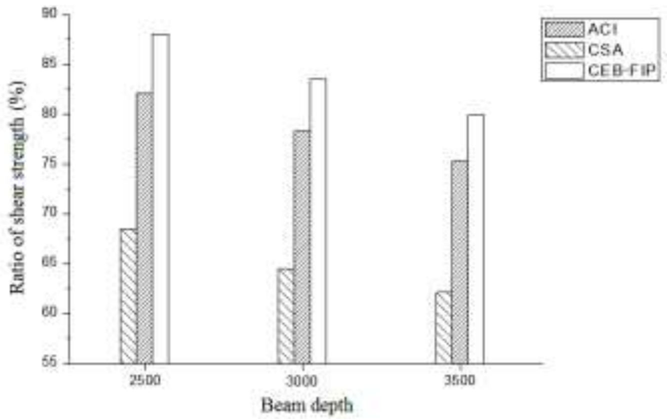

Figure 2. Shear strengths estimated by the current design codes for different aspect ratios of beam cross section.

TABLE IV. RATIOS BETWEEN THE SHEAR STRENGTHS PREDICTED BY THE THREE CURRENT CODE PROVISIONS AND THE SHEAR STRENGTH EQUATIONS FOR THREE DIFFERENT BEAM DEPTHS.

Beam depth (mm)	**2,500**	**3,000**	**3,500**
ACI	82.1 %	78.3 %	75.3 %
CSA	68.5 %	64.4 %	62.1 %
CEB-FIP	88.0 %	83.5 %	79.9 %

TABLE V. RATIOS BETWEEN THE SHEAR STRENGTHS PREDICTED BY THE THREE CURRENT CODE PROVISIONS AND THE SHEAR STRENGTH EQUATIONS FOR THREE DIFFERENT AMOUNTS OF MAIN REINFORCEMENT.

(a) $A_s = 7{,}800$ mm^2.

Shear-span ratio	**0.6**	**1.0**	**1.5**
ACI	S	F	F
CSA	S	S	S
CEB-FIP	F	F	F

(b) $A_s = 9{,}100$ mm^2.

Shear-span ratio	**0.6**	**1.0**	**1.5**
ACI	S	F	F
CSA	S	S	S
CEB-FIP	S	F	F

(c) $A_s = 10{,}500$ mm^2.

Shear-span ratio	**0.6**	**1.0**	**1.5**
ACI	S	S	S
CSA	S	S	S
CEB-FIP	S	F	F

Lastly, the effect of the amount of main reinforcement on the shear strength is investigated. Table V shows the failure modes of the representative example for three different amounts of main reinforcement, which are 7,800 mm^2, 9,100 mm^2 and 10,500 mm^2. The beam depth is 2,500 mm for all these cases. In the table, 'S' represents the case where the inclined concrete strut reaches its strength earlier than the other strut and tie components, and 'F' indicates the case where the horizontal tie reaches its strengths earlier than the other components. Therefore, 'S' and 'F' correspond to the general shear and flexural failures, respectively. By comparing the three sub-tables in Table V, two observations can be made. First, the governing failure mode changes from shear failure to flexural failure as shear-span ratio increases. Second, the CSA code underestimates the concrete strut strength, thus only shear failure occurs. In contrast, CEB-FIP code relatively overestimates it, thus shear failure is difficult to occur even in the case of large amount of main reinforcement.

V. Conclusions

This paper investigated the validity of the three current concrete design codes, which are ACI 318-11, CSA A.23.3-04 and CEB-FIP Model Code 2010, on these issues by comparing the estimates by the code with those of the strength equations by Hong et al. The main conclusions of this paper are as follows:

1) The comparison shows that the current ACI and CEB-FIP design codes can provide reasonable shear strength estimates that approximately correspond to the 70 to 80 % of the predictions by the shear strength equations. In contrast, the current CSA code relatively underestimates the shear strength for cases with large shear-span ratio.

2) The shear strength estimates by the current design codes based on the single-span truss model may not be accurate if the aspect ratio of beam cross section is large.

3) The governing failure mode changes from shear failure to flexural failure as shear-span ratio increases, and flexural failure is difficult to occur for cases with large amount of main reinforcement.

Acknowledgment

This research was supported by Basic Science Research Program through the National Research Foundation of Korea (NRF) funded by the Ministry of Science, ICT & Future Planning (2011-0011078).

References

[1] S.G. Hong, D.-J. Kim, S.Y. Kim, and H.N. Kim, "Shear strength of reinforced concrete deep beams with end anchorage failure," ACI Structural Journal, vol. 99, pp.12-22, January 2002

[2] American Concrete Institute, ACI Committee 318, Building code requirements for structural concrete and commentary, 2011, p. 465.

[3] CSA A23.3-04, Design of concrete structures, Canadian Standards Association, Muktha Tumkur, 2004, p. 214.

[4] Siegmar Kästl e.K, The International Federation for Structural Concrete, CEB-FIP model code, 2010, p.53.